Araştırma Makalesi / Research Paper
Bayburt Üniversitesi Fen Bilimleri Dergisi
Bayburt University Journal of Science

dergipark.gov.tr/bufbd
ISSN: 2667-579X

Cilt 6, Sayı 1, Yıl 2023, Sayfa 71-88
Vol 6, Issue 1, Year 2023, Pages 71-88
doi.org/10.55117/bufbd.1282591

Geliş Tarihi / Date of Recieve: 13.04.2023
Revizyon Tarihi / Date of Revision: 17.05.2023
Kabul Tarihi / Date of Acceptance: 22.05.2023

An Experimental Study on the Determination of Minimum Fluidization Velocity

Alperen TOZLU[1*], Ahmet İhsan KUTLAR[2], Melda ÖZDİNÇ ÇARPINLIOĞLU[2]

[1]*Bayburt University, Department of Mechanical Engineering, 69000, Bayburt, Turkey*
[2]*Gaziantep University, Department of Mechanical Engineering, 27310, Gaziantep, Turkey*

Keywords:

Pneumatic conveying systems, Flow modes, Particle classifications, Minimum fluidization velocity

Abstract

Pneumatic conveying systems are widely used in a variety of industrial settings since different types of materials can be conveyed. There are some classifications of flow modes for conveying of powders and bulk solid particles based on mean particle size, density, and inter particle cohesion forces. In this paper, three different cases which are vertical (test case 1), horizontal (test case 2) and continuous conveying test case are constructed and considered in order to determine the flow modes in pneumatic conveying systems. Seven solid particles are used with the range of 200 kg/m^3 < ρ_{blp} < 2400 kg/ m^3 and 150 µm < d_p < 2750 µm in these three cases. In vertical test set-up unstable zone and fluidized dense phase is occurred, then in the horizontal test set-up slug flow and plug flow is observed and lastly plug flow and dilute phase is occurred visually in continuous conveying test case. Finally, all obtained data are considered for the classification according to flow modes in pneumatic conveying systems. The observed flow modes are considered and tabulated with respect to all test cases.

*e-mail: alperentozlu@bayburt.edu.tr

Bu makaleye atıf yapmak için:
Alperen TOZLU; Ahmet İhsan KUTLAR; Melda ÖZDİNÇ ÇARPINLIOĞLU, "Minimum Akışkanlaştırma Hızının Belirlenmesi Üzerine Deneysel Bir Çalışma", Bayburt Üniversitesi Fen Bilimleri Dergisi, C. 6, s 1, ss. 71-88

How to cite this article:
Alperen TOZLU; Ahmet İhsan KUTLAR; Melda ÖZDİNÇ ÇARPINLIOĞLU, "An Experimental Study on the Determination of Minimum Fluidization Velocity", Bayburt University Journal of Science, vol. 6, no 1, pp. 71-88

1 INTRODUCTION

Pneumatic conveying systems are widely used in various industrial settings due to the spectrum of materials to be conveyed. Basically, it becomes important phenomenon in decision stage of the effective flow modes to reduce the required energy for conveying of any particles in well-designed conveying pipeline systems in industry. There are some classifications of flow modes for conveyed both powders and bulk solid particles based on mean particle size and density difference, and also by taking into account inter particle cohesion forces. Pneumatic conveying systems are quite simple to setup in a factory such as chemical, food, textile, pharmaceutical industries etc. Gas velocity, gas flow rate, minimum fluidization velocity, particle size, particle density, bulk density and particle shape are the most important parameters used to identify a two-phase flow mode. In practice, non-suspension or dense phase flow is desirable for measure of conveying in terms of the ratio of conveyed material in amount to the amount of air supply whereas the suspension or dilute phase flow is not. However, many products have to be conveyed in dilute phase conveying system. Particle/air interaction parameters such as permeability, air retention and de-aeration are all dependent on physical properties of conveyed materials such as: particle size, size distribution, density of particle, loose-poured bulk density and shape. Loose-poured bulk density, ρ_{blp}, of bulk materials is the mass per unit volume which is measured when particle is in a loose, non-compacted or poured condition, expressed as follows:

$$\rho_{blp} = (1-\varepsilon)(\rho_s - \rho_g) \tag{1}$$

where ρ_s is density of solid particle conveyed, ρ_g is fluid density and ε is bulk voidage.

Permeability, P_f is a measure of how the air flows through the material under a motive force and can be expressed as ratio of superficial velocity of gas, U to pressure drop per unit pipe length, $\Delta P/L$ occurring in flow line:

$$P_f = U/(\Delta P/L) \tag{2}$$

Superficial gas velocity, U is defined as:

$$U = Q/A \tag{3}$$

where Q is volumetric gas flow rate and A is cross-sectional area of bed/pipe.

Air retention is the ability of a material to retain air in the void spaces of the material after the air supply has been terminated. De-aeration, A_f is a measure of how the air naturally escapes from the material and can be expressed as;

$$A_f = t(\Delta P/L) \tag{4}$$

where t is the time related to the pressure drop decay plot from fluidization pressure to atmospheric pressure. Minimum fluidization velocity, U_{mf} at the onset of fluidization is commonly given as;

$$U_{mf} = P_f\, m_f(\Delta P/L) \tag{5}$$

An aerated state of a substance is referred to as fluidization. When air velocity drops below the minimum conveyance value, a process known as saltation, which involves the deposition of particles along horizontal pipelines, takes place. The term "dense phase" (also known as "non-suspension") refers to a state in which the particle-conveying gas velocity is lower. Another typical condition that might happen when gas velocity equals or exceeds the particle saltation velocity is the diluted phase (suspension). The presence of liquid-rich slugs that cover the whole channel or pipe region is referred to as slug flow. It is appropriate to use this type of flow to transport friable and/or granular items. Some transported particles aggregate at the bottom of the pipeline and create lengthy plugs when the air mass flow rate is lowered. Plug flow is the term used to describe the flow we just discussed. Due to the creation of lengthy plug structures, large pressure changes in plug flows may result in vibration in entire systems. It is known as an unstable zone in this area. In order to significantly reduce costs, it would be preferable to employ a suitable prediction method to detect flow modes during the design stage of a pneumatic conveying system rather than relying just on experimental work. Instead than testing transporting material in a pipeline at the outset of design, it is more convenient to discover modes of flow using some predictive techniques, offering a significant economic benefit. There are two different classifications used in the literature to create generalized flow charts: one based on the physical characteristics of the particles transported [1-3] and the other based on the particle/air interaction of the gas-solid phase [4–9]. A loose-poured bulk density parameter [10–14] and inter-

particle cohesion forces [15] are also taken into account when improving the classifications based on the physical characteristics of the particles.

In terms of mean particle size and density difference, Geldart [1] divided the gas-solid flow character into four types. This classification can be summed up as follows: i) Powders in Group A that exhibit dense phase expansion following minimal fluidization are those with small mean sizes and/or low particle densities (less than roughly 1.4 g/cm^3). ii) Powders in Group B will bubble at minimum fluidization velocity in contrast to powders in Group A. The materials in this group have mean size and density ranges of 40μm≤ dp≤500μm and 1.4g/cm3≤ ρs ≤4g/cm3, respectively. iii) Group C powders are difficult to fluidize at all because of the interparticle cohesive forces. The powder lifts as a plug in small diameter tubes, or channels (rat-holes) negatively. The interparticle forces are higher than the fluid forces exerted on particle. iv) The materials in Group D have comparatively large and/or very dense particles. The materials in this group can be spouted if gas is admitted only through a centrally positioned hole.

In addition to Geldart's classification, Molerus [4-6] took interparticle cohesive forces into consideration. By examining the forces, the gas exerts on the particles and the cohesive forces between particles, semi-empirical criteria were used to determine the limiting conditions between Group A-C, Group A-B, and Group B-D. In Geldart's diagram, there is no separation between Group A and Group C. However, Molerus [4-6, 16-21] proposed an equation describing the boundary between Group A-C for hard particles as;

$$D_{1max}/F_T = 10(\rho_s - \rho_g)\, d_p^3 g/F_H = K_1 = 1/100 \quad (6)$$

where D_{1max} is maximum drag force, F_T is average tensile force transmitted per particle, F_H is adhesion force transmitted in a particles contact. Molerus [5] also defined an equation describing Group A-B boundary for hard particles as follows;

$$(\rho_s - \rho_g)\pi d_p^3 g/6F_H = K_2 = 0.16 \quad (7)$$

To predict the Group B-D boundary, the following equation is proposed by Molerus [5];

$$(\rho_s - \rho_g) d_p g = 15.3 \quad (8)$$

Dixon [3] classified gas-solid flows into three groups as i) axisymmetric slugs, ii) weak asymmetric slugs (dunes) and iii) no slugs at all. He considered the relationship between the gas slug velocity, U_{sp}, terminal velocity, U_t, and minimum fluidization velocity, U_{mf} using the following equations;

$$U_{sp} = 0.35(K_{sp} g D)^{1/2} \quad (9)$$

where D is pipe diameter and =1 for axisymmetric slugs; =2 for asymmetric slugs.

$$U_t = 0.152(\rho_s - \rho_g)^{0.714} d_p^{1.14} g^{0.714} / \mu^{0.428} \rho_g^{0.258} \quad (10)$$

$$\rho_s (1-\varepsilon) = 150 (1-\varepsilon)^2 (\mu\, U_{mf})/(\varepsilon^3 g.d_p^2) + 1.75(1-\varepsilon)(\rho_g U_{mf}^2)/(\varepsilon.g.d_p) \quad (11)$$

where ε is voidage which is ratio of space volume among particles/powders in a bed to total volume of bed. According to Dixon [3], there is no stable slug formation if $U_t < U_{sp}$ hence the boundary between no slugging and asymmetric slugs is denoted at $U_t = U_{sp}$. No full bore plug flow occurs if $U_{mf} < U_{sp}$ hence the boundary between axisymmetric slug and weak asymmetric slugs is given by $U_{mf} = U_{sp}$. Mainwaring and Reed [7] presented his experimental work in the form of two diagrams as a function of permeability and de-aeration factors of materials tested with respect to steady state fluidization pressure drop per unit length for dense phase conveying at minimum fluidization. Mainwaring and Reed [7] proposed the limit line separating two modes of fluidized dense phase and plug flow by introducing a new parameter defined as m^{3}s/kg. Fargette et al. [8] classified the powders conveyed in a dense phase, which are particularly used in steel manufacturing process, based on the permeability factor, air retention and cohesion of powders. They defined the pneumatic flow parameter, Ω as follows:

$$\Omega = t_{da}/\rho_{blp}\, P_f \quad (12)$$

If $\Omega > 4000$, the mode of flow becomes fluidized dense phase; plug flow if $\Omega < 18$ and flow is dilute only if $18 < \Omega < 4000$.

Chambers et al. [22] introduced a parameter similar to that of Fargette et al. [8], but now N_c is based on permeability, de-aeration time and particle density instead of loose-poured bulk density, as;

$$N_c = \rho_s P_f / t_{da} \quad (13)$$

Materials conveying was divided into three flow types by Chambers et al. [22]: dense phase slugging mode, lean phase mode, and dense phase moving bed mode. The conveyed material is appropriate for slugging dense phase transportation for $N_c>0.01$; and for $N_c<0.001$, the material can be conveyed as a dense phase conveying in a moving bed flow. At intermediate range of $0.001<N_c<0.01$, the material can be conveyed only in a lean phase mode. By evaluating and contrasting the various methodologies described in the literature, Sanchez et al. [9, 23–28] were able to forecast the viability of conveying particles in dense phase mode by taking into account the measurement of the permeability and de-aeration time of the particles. They used their fluidization equipment to perform the measurements for the permeability factor and the de-aeration parameter. The primary parameters, such as particle size, shape, bulk density, permeability, de-aeration, cohesiveness, etc., and the secondary parameters, such as adhesion, moisture, electrostatics, elasticity, and temperature sensitivity, were classified by Sanchez et al. [9] into two general groups. It is discovered through categorization that some materials do not adhere to Geldart's classification when the secondary factors are considered. Then a group of dimensionless parameters were defined and results were presented in terms of these dimensionless parameters such as de-aeration factor, permeability factor and Froude number based on minimum fluidization velocity as;

$$Grt = \mu t_{da} / d_p (\rho_s + \rho_g /2) \quad (14)$$

$$P^* = P_f \rho_s (g d_p)^{1/2}/d_p \quad (15)$$

$$Fr_{mf} = U_{mf} /(g d_p)^{1/2} \quad (16)$$

Using the ρ_{blp} rather than the distinction between particle and gas densities, Pan [13] amended Geldart's classification and divided the flow in conveying bulk solid materials into three modes: A smooth transition from the diluted to fluidized dense phase is represented by PC1; an unstable zone and slug flow are represented by PC2; and the diluted phase is only taken into account by PC3 when it comes to pressure drop and air mass flow rate. Williams and Jones [14] examined the classification diagrams of Geldart, Molerus, and Dixon and changed the particle density parameter there with ρ_{blp} in their charts. On the basis of the basic particle parameter and the air-particle parameter, Jones and Williams [15-29] have developed two different types of predictive charts. The first attempt at improvement was switching out the particle density utilized in the prediction parameter procedures for loose-poured bulk density. An air-particle based technique was improved such that in the new scheme there is no necessary of use of any de-aeration parameter. The equations which describe these boundaries between the fluidized dense phase and dilute only Eqn. 17, and dilute only and plug flow Eqn. 18 were introduced as follows;

$$P_f \rho_{blp}^{3/4} \approx 300 \quad (17)$$

$$P_f \approx 20x10^{-6} \quad (18)$$

They also modified Chambers et al.'s parameter as follows;

$$P_f \rho_s /t_c = Nc_{(mod)} \quad (19)$$

where t_c is de-aeration time as defined by Jones [15] and Sanchez [9]. If $Nc_{(mod)}$<8x10-4, flow is fluidized dense-phase. It is dilute only when 8x10-4 < $Nc_{(mod)}$<0.07 and plug flow if $Nc_{(mod)}$>0.07.
It might be claimed that Geldart's [1] classification helps with pneumatic conveying system flow mode estimation. However, it cannot be used in isolation to predict the flow mode in the dense phase. Additionally, Dixon's [3] method is practical during the design phase but is only provisional for a precise prediction of flow modes. Because permeability and de-aeration parameters are included in the Mainwaring and Reed's [7] approach rather than depending just on the physical characteristics of the particles, it is a more accurate predictive method than the Geldart's [1] and Dixon's [3] approaches. Fargette et al. [8] introduced a non-dimensional parameter made up of de-aeration time, permeability, and ρ_{blp} to take the air/particle interaction into account. Another dimensionless parameter, similar to that suggested by Fargette et al. [8], was also developed by Chambers [22] utilizing particle density rather than loose poured bulk density. Some materials, according to Sanchez [9], do not conform to Geldart's[1] classification because of their secondary parameter values. By taking into account cohesive forces, Molerus [5] changed Geldart's [1] classification and also described the criterion between Geldart's [1] Group A-C. According to ρ_{blp} and median particle diameter, Pan [13] sorted the flow mode and found that his results agreed with those of Geldart [1], Dixon [3], Mainwaring and Reed [7], and others. By considering ρ_{blp} and P_f, Jones and Williams [15] analysed all works that were available for their study and also offered new standards for Geldart's [1] Groups A–B and B–D.

Table 1. Summary of proposed criteria in terms of modes of flow in pneumatic conveying systems

Authors	Modes of flow	Predictive diagrams	Limitations	Boundaries and formulations
Geldart [1]	A-Fluidized dense-phase	Particle density difference - mean particle diameter (kg/m^3) - (m)	ρ_s < 1.4 gr/cm^3	A/C-B $\left(\rho_s-\rho_g\right)d_p = 225x10^{-3}$
	B- Dilute phase		ρ_s >1.4 gr/cm^3 $500\mu m > d_p > 40\mu m$	
	C- Difficult to fluidize		Difficult to fluidization	B-D $\left(\rho_s-\rho_g\right)d_p^2 = 10^{-3}$
	D- Plug mode of dense phase		Large or dense particles	
Dixon [3]	Axisymmetric slugs- Plug type	Particle density difference - mean particle diameter (kg/m^3) - (m)	-	Axissymettric/asymmetric $\frac{d_p\left(\rho_s-\rho_g\right)}{D^{0.5}} = \frac{1.64x10^{-3}}{d_p} + 2.68D^{0.5} - \frac{\rho_g d_p}{D}$
	Weak asymmetric slugs- Dilute phase		$V_{mf} < V_{sp}$ (m/s)	
	No slugging- Fluidized dense-phase		$V_t < V_{sp}$ (m/s)	No slugging/asymmetric $\frac{d_p^{1.14}\left(\rho_s-\rho_g\right)^{0.714}}{D^{0.5}} = 136x10^3$
Mainwaring and Reed [4]	Plug type	Permeability- $(\Delta P/L)$	V_{mf} >50 mm/s	$V_{mf} = P_f\left(\frac{\Delta P}{L}\right)_{ss} = 50mm/s$
	Dilute only or fluid. dense-phase		V_{mf} <50 mm/s	
	Fluidized dense phase	De-aeration/density- $(\Delta P/L)$	X>0.001m^{2}s/kg	$\frac{\Delta P}{L}X = \frac{A_f}{\rho_s}$
	Dilute only or plug flow		X<0.001m^{2}s/kg	
Fargette et al. [5]	Fluidized dense phase	Non-dimensional parameter (Ω)	Ω >4000	$\Omega = \frac{t_{da}}{P_f\rho_{blp}}$
	Dilute only		18< Ω <4000	
	Plug flow		18< Ω	
Chambers et al. [6]	Dense-phase/moving bed	Non-dimensional parameter (N_c)	N_c <0.001	$N_c = \frac{\rho_s P_f}{t_{da}}$
	Lean phase mode		0.001< N_c <0.01	
	Slugging dense-phase		N_c >0.01	
Sanchez et al. [7]	Fluidized dense phase	Non-dimensional parameters: Grt, P^*, Fr_{mf}	Grt >0.2x10^{-3}	$Grt = \frac{\mu}{d_p\left(\rho_s+\rho_g/2\right)t_{da}}$ $P^* = \frac{P_f\rho_s\sqrt{gd_p}}{d_p}$ $Fr_{mf} = V_{mf}/\sqrt{gd_p}$
Molerus [8]	Geldart's A-Fluid. dense-phase	Particle density difference - mean particle diameter (kg/m^3) - (m)		
	Geldart's B- Dilute phase			A-C (for hard particles) $10\frac{\left(\rho_s-\rho_g\right)d_p^3 g}{F_H} = 0.01$
	Geldart's C-Difficult to fluidized			A-B (for hard particles) $\frac{\left(\rho_s-\rho_g\right)\left(\pi d_p^3 g/6\right)}{F_H} = 0.16$
	Geldart's D- Plug flow			B-D $\left(\rho_s-\rho_g\right)d_p g = 15.3$
Pan [9]	PC1- Fluidized dense-phase	Loose poured bulk density-Mean particle diameter (kg/m^3) - (μm)	-	PC1-PC2/3 $d_p\rho_{blp} = 0.1206$
	PC2- Unstable zone- slug flow-dilute phase		$d_p > 1000\mu m$	
	PC3 Dilute only		-	PC2-PC3 $\rho_{blp} = 1000$
Williams & Jones [10]	Geldart's A-	Loose poured bulk density-Mean particle diameter (kg/m^3) - (μm)		A/C-B $\rho_{blp}d_p = 121x10^{-3}$
	Geldart's B- Dilute phase			
	Geldart's C-			B-D $\rho_{blp}d_p^2 = 539x10^{-6}$
	Geldart's D- Plug flow			
	Dixon's Axisymmetric slugs- Plug type			Asym. slugs - axisymmetric slugs $\frac{d_p\rho_{blp}}{D^{0.5}} = \frac{0.885x10^{-3}}{d_p} + 1.44D^{0.5}$
	Dixon's Weak asymmetric slugs- Dilute only			
	Dixon's no slugging- Fluidized dense-phase			No slugging-asymmetric slugs $\frac{d_p^{1.14}\rho_{blp}^{0.714}}{D^{0.5}} = 87.4x10^3$
	Molerus's A-			A/C-B $\rho_{blp}d_p^3 = 1.27x10^{-9}$
	Molerus's B-			
	Molerus's C-			B-D $\rho_{blp}d_p = 0.841$
	Molerus's D- Plug flow			
Jones & Williams [11]	Chambers – Fluid. dense-phase	Non-dimensional parameter $(N_{c(\mathrm{mod})})$	$N_{c(\mathrm{mod})}$ <8x10^{-4}	$N_{c(\mathrm{mod})} = \frac{\rho_s P_f}{t_c}$
	Chambers – Dilute only		8x10^{-4}< $N_{c(\mathrm{mod})}$ <0.07	
	Chambers – Plug flow		$N_{c(\mathrm{mod})}$ >0.07	
	Fluidized dense-phase	Loose poured bulk density-permeability (kg/m^3) - (m^{3}s/kg)		$P_f\rho_{blp}^{3/4} \approx 300$
	Dilute only			$P_f \approx 20x10^{-6}$
	Plug flow			

Therefore, from Geldart's method [1] to the work of Jones and Williams [15], there are numerous flow mode diagrams and proposed criteria to utilize in determining flow modes for pneumatic conveying of powders/granular particles. As it can be seen, some of the scientists considered only physical properties of particles/powders while others took into account both physical properties of particles and air/particle interaction. There are some agreements and conflicting results among the proposed approaches. Thus, all proposed criteria are reviewed and sorted out by Tozlu et. al. [30] for further studies and also the available classifications of modes of flow for pneumatic conveying of powders and granular particles are summarized as shown in Table 1[31-34].

2 EXPERIMENTAL TEST SET-UP AND METHODOLOGY

The vertical test set-up is designed in order to determine the minimum fluidization velocities. On the other hand horizontal test set-up is constructed for investigation of flow dynamics during pneumatic conveying of a variety of particles and their effects such as mass, density, size etc. The vertical test set-up, vertical test chamber, and horizontal test set-up are shown in Figure 1, Figure 2, and Figure 3 respectively.

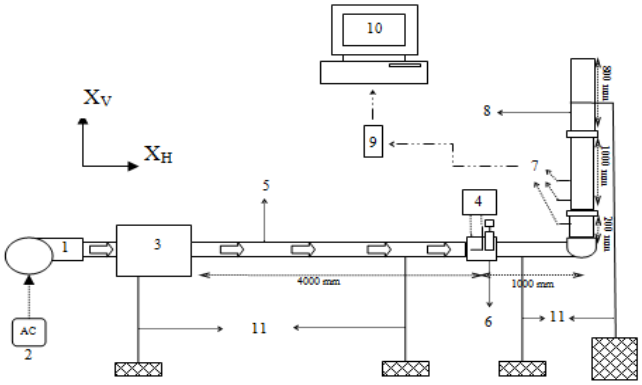

1. Blower unit 2. AC control unit 3. Settling tank 4. Manometer 5. PVC pipe 6. Pitot-tube and traverse mechanism
7. Pressure Transmitter 8. Acrylic glass pipe 9. Daq board 10. PC 11. Supports

Figure 1. Vertical test set-up

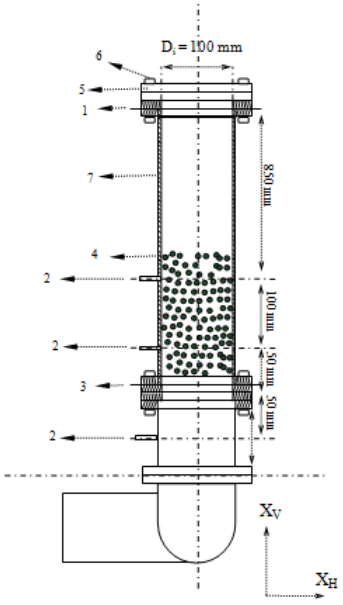

1. Upper perforated plate 2. Pressure transmitters 3. Lower perforated plate 4. Solid particles
5. Flange plate 6. Screw 7. Acrylic test chamber

Figure 2. Vertical test chamber

The reference test section is located at XR/D = 38.46 from the exit section of the settling tank. At this reference measurement section, the flow is found to be fully developed one for all test runs. Three pressure transmitters (WIKA SL-1) are used in vertical test set-up and four pressure transmitters are used which in horizontal test set-up. Particle feeder is to induce solid particles into air flowing through the pipeline system in horizontal test set-up.

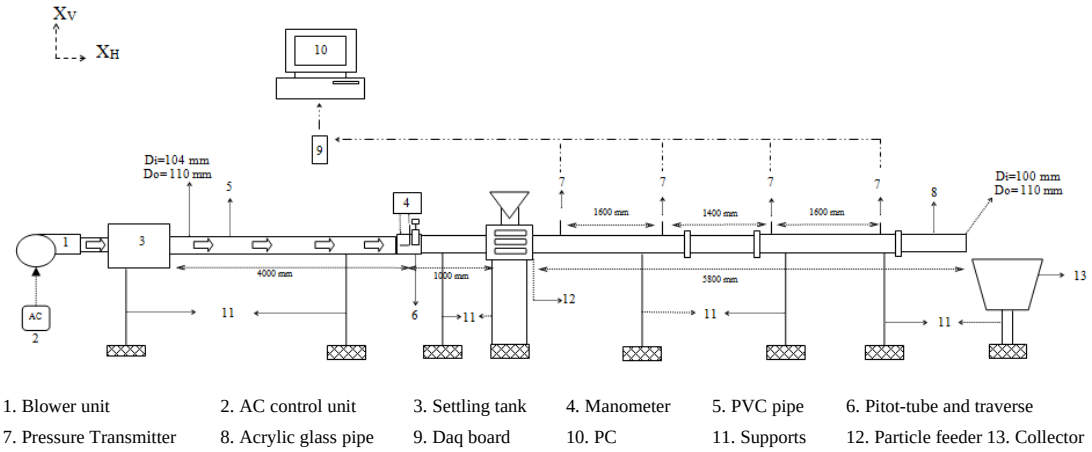

Figure 3. Horizontal test set-up

A pitot tube and a traverse mechanism is mounted at X_R/D=38.46 downstream of the exit part of settling tank. A 16-bit, 1-MHz A/D converter (NI USB-6353 X series DAQ, USB Board with 32 single-ended, 48 differential analog inputs and 4 analog outputs) is used in order to collect the pressure data. NI USB-6353 X series DAQ, USB daq board is instructed by a LabView software program. The data is collected by using a devised program which is named as FDRIPCS.vi (Flow Dynamics Research in Pneumatic Conveying System) in LabView 2009SP1® environment.

Sizes of solid particles are categorized by a custom design sieve with eight different meshes which have diameters of 0.1 mm, 0.4 mm, 1.0 mm, 1.25 mm, 1.5 mm, 2.0 mm, 2.5 mm and 3.0 mm. The average particle diameter, d_p is taken as %50 of the weight of sieved particles. The densities of particles ρs are calculated with custom design sieve and the ρ_{blp} densities are determined by following ASTM standard code B212-76 [35]. The relation between loose-poured bulk density ρ_{blp}, particle density ρ_s and voidage ε, is given in Eqn. 20:

$$\rho_{blp} = (1-\varepsilon)\,\rho_s \tag{20}$$

Seven different type solid particles are used at the test runs and they are categorized with respect to their loose-poured bulk densities and sizes as shown in Table 2.

Table 2. Physical characteristics of solid particles

Particle	Code	Size range (μm)	d_p (μm)	Shape	ρ_s (kg/m^3)	ρ_{blp} (kg/m^3)	(ε)
Semolina	SE	400-1000	700	Roughly spherical	1459	850	0.417
Wheat	W	2000-2500	2250	Roughly spherical	1356	950	0.299
Polyethylene	PE	2500-3000	2750	Roughly spherical	910	550	0.396
Zeolite 1	Z1	100-400	250	Roughly spherical	1450	1000	0.45
Zeolite 2	Z2	400-1000	700	Roughly spherical	1450	920	0.365
Sand (Garnet)	S	150	150	Roughly spherical	4110	2400	0.416
Tea Flakes	T	1250-1500	1375	Filament	433	200	0.538

3 RESULTS AND DISCUSSION

3.1 Determination of Minimum Fluidization Velocity

There is no exact determination for the minimum fluidization velocity in the literature. In the vertical test set-up, solid particles are used with three different bed lengths (10 mm, 30 mm and 50 mm) in the form of a cylindrical bed in a vertical test chamber symbolizing L10, L30 and L50 respectively. The experimental study is conducted by measuring the local static pressures in the vertical test chamber at varying air flow rates with the range of 3.65 m/s < U_{air} < 24.83 m/s. At each U_{air} the field is observed with the measurement of the local static pressures the

preliminary experiments; measurements indicate that variation of local static pressures at X_V/D= 1.5, 2.5, 3.5 and 8.5 which can be used as a determination tool for the flow inside. The measurements of local static pressures at P_2 is given as a function of P_1 for different U_{air} with the range of 3.65 m/s < U_{air} < 24.83 m/s in Figure 4.

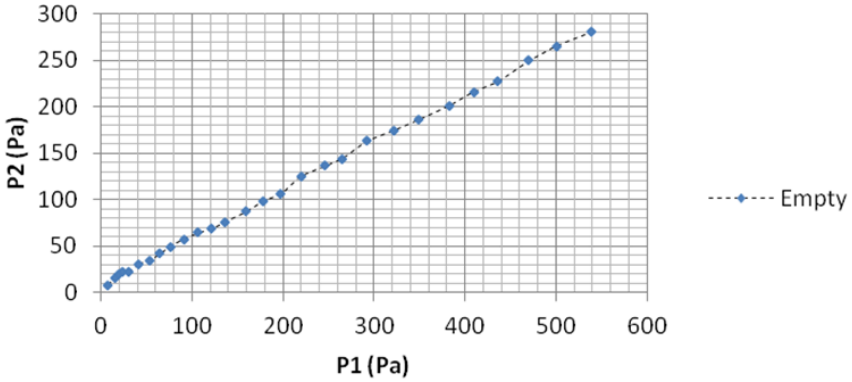

Figure 4. Local static pressure variation in empty pipe in vertical test set-up

The visual observation for the minimum fluidization state is verified by the local static pressure measurements, the static pressure at before the bed X_V/D= 1.5 is called as P_1 and the static pressure at X_V/D= 2.5 after the bed is called as P_2. In the experiments the local static pressures at location $X_V/D > 2.5$ defined as P_3 and P_4 have no effects on state. Therefore, variation of P_1 and P_2 is used for the state determination.
Measurement of local static pressures along the horizontal test set-up is conducted in empty pipe. Local static pressures are given as a function of U_{air} for empty pipe in Figure 5.

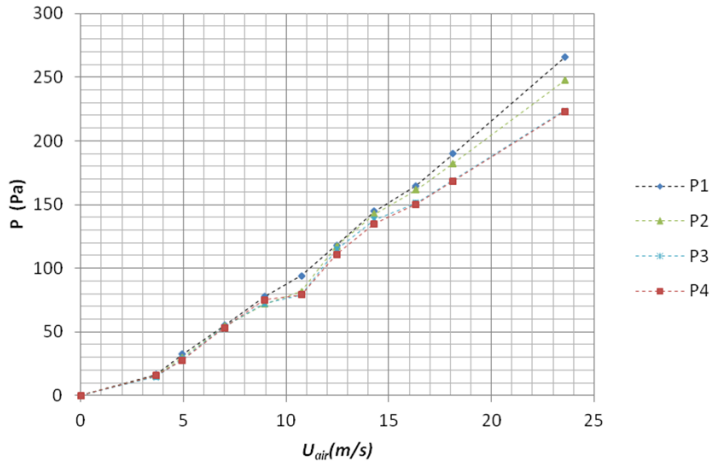

Figure 5. Local static pressure variation in empty pipe in horizontal test set-up

A horizontal bed in the form of a prismatic configuration with the use of SE, S, W, T and PE was located at the position X_H/D= 10. The air flow velocity U_{air} is changed gradually in the range of 3.65 m/s < U_{air} < 24.83 m/s. At each U_{air} the field and structure of particles configuration is visually observed. The measurements of local static pressures P_1 at X_H/D= 2 before the prismatic configuration and P_2 at X_H/D= 18, P_3 at X_H/D= 32 and P_4 at X_H/D= 48, after the configuration are used to analyze the minimum fluidization state. The experiment is performed with the increase of U_{air}, 3.65 m/s < U_{air} < 24.83 m/s. So that, the distribution of solid particles is observed and also local static pressures P_1, P_2, P_3 and P_4 are determined with the aid of pressure transmitters and recorded.

In the horizontal test set-up visual observation of prismatic configuration of solid particles is also analyzed by determining flow dynamics through the measurement of amount of mass, $\dot{M}_p$ transported at each U_{air}. The collected amount of $\dot{M}_p$ is measured by recording time with collection through assay balance at the end of the horizontal test section. In order to deduce about the influence of particle characteristics results on minimum fluidization velocity are given in a comparative base.

For the final test set-up, a sample dynamic verification experimental study is conducted. This test based upon the experimental measurements of the first and second test cases in order to complete flow mode analysis. In this test set-up, three solid particles which are S, W and SE are used to observe flow modes during the continuous

conveying with particle feeder. The particle feeder induced the known amount of particles into the pipeline system with determined mass flow rates, $\dot{m}_p$. Particle feeder induces different $\dot{m}_p$ of particles (S, SE, W) into the air flow pipeline. The measurements of local static pressures at defined points through the horizontal line after the particle feeder are measured together with the amount of particle transported by air. The measurements are started at the maximum U_{air} to observe a fully suspended-dilute phase inside the horizontal test section. The measurements are repeated by reducing U_{air}. At each U_{air} the measurements together with visual observation of the test section are used for flow mode analysis. The least; U_{air} at no particle conveying point is also referred to determine a critical state for the flow mode. Therefore, the flow field observation with the static pressure measurements is compared with vertical and horizontal test set-up.

3.2 Results in the Vertical Test Set-up

The minimum fluidization velocities, U_{mf} of seven different particles of SE, S, W, T, Z1, Z2 and PE are given in Table 3 in case of different flow rates from 0.029 m^3/s to 0.195 m^3/s. U_{mf} is not observed for S particles at L50.

Table 3. Minimum fluidization velocities corresponding to the visual observation of the shape

Particles	U_{mf} (m/s)	Air Flow Rate (m^3/s)	Particles	U_{mf} (m/s)	Air Flow Rate (m^3/s)
Z1 (10 mm)	7.44	0.058	S (30 mm)	21.70	0.170
Z1 (30 mm)	15.87	0.125	SE (10 mm)	6.99	0.055
Z1 (50 mm)	21.70	0.170	SE (30 mm)	17.38	0.136
Z2 (10 mm)	8.42	0.066	SE (50 mm)	21.70	0.170
Z2 (30 mm)	17.38	0.136	PE (10 mm)	7.89	0.062
Z2 (50 mm)	23.56	0.185	PE (30 mm)	13.81	0.108
W (10 mm)	9.89	0.078	PE (50 mm)	18.13	0.142
W (30 mm)	18.13	0.142	T (10 mm)	3.65	0.029
W (50 mm)	24.83	0.195	T (30 mm)	8.20	0.064
S (10 mm)	6.17	0.048	T (50 mm)	11.22	0.088

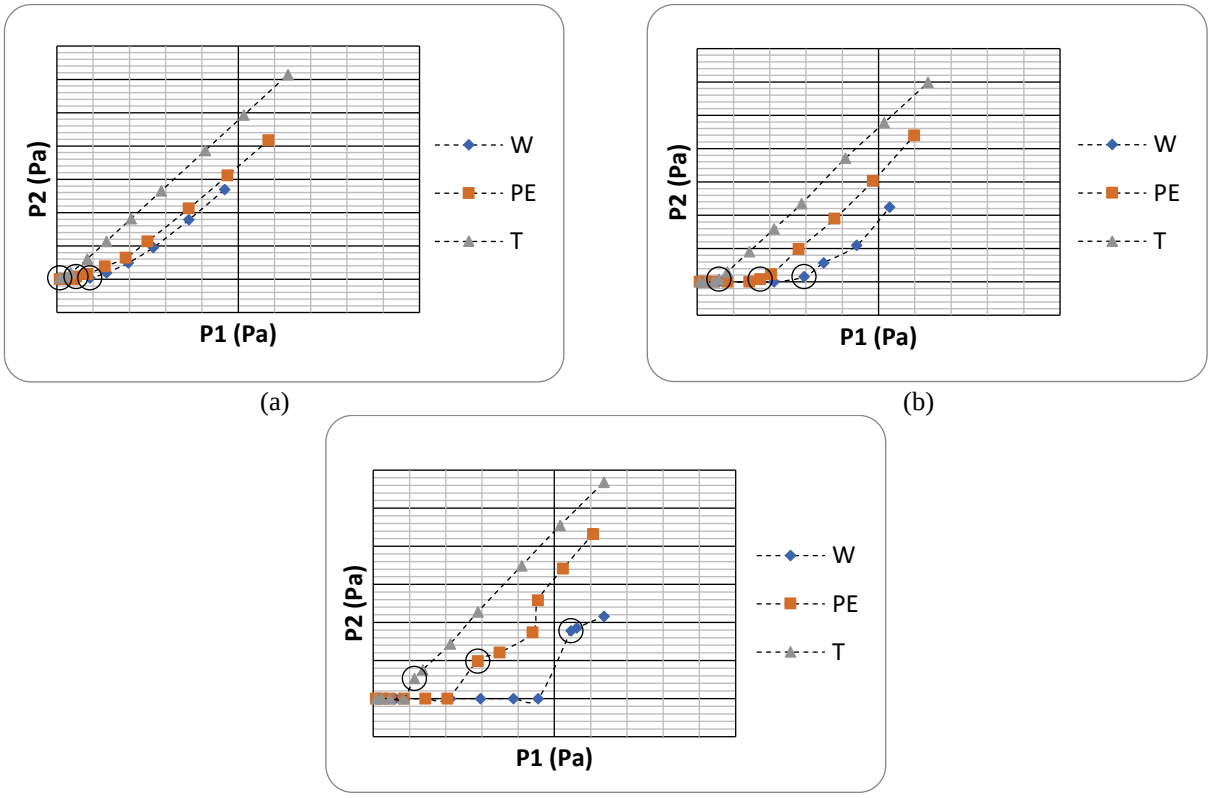

Figure 6. Pressure variation for W, PE and T at (a) L10, (b) L30, and (c) L50

For each test case, vertical test chamber is filled with particles to the desired bed length and blower is operated until all particles in vertical test chamber are just suspended in which this phenomenon is called as start to fluidization. At this time, U_{air} is measured by using pitot tube at the reference test section. This U_{air} is taken as minimum fluidization velocity. At the same time, static pressures are measured and acquired by means of a devised program. After the observation of U_{mf}, the fan speed is increased systematically up to the maximum flow rate of 0.207 m^3/s until the flow becomes fully suspended. U_{mf} values is found in the range of 3.65 m/s < U_{mf} < 24.83 m/s. The minimum and maximum U_{mf} values are found for T particles at L10, and W particles at L50 respectively.
P_1 and P_2 are calculated for each bed lengths which are shown in Figure 6a, 6b, and 6c for L10, L30, and L50 respectively. As shown in Figure 6, although the value at P_1 increases continuously due to increase in air flow rate, the value of P_2 is seen to be zero up to minimum fluidization velocity is obtained. When the particles just begin to bubble, the value of P_2 begins to increase. In Figure 6, three particles are given due to a wide range of ρ_{blp}. The results showed that the particle which have lower ρ_{blp} fluidizes earlier then the heavier ones.

Bed length is governing parameter on U_{mf} determination for all particles. This influence is dominant in comparison with the corresponding effect of L for PE and T. As can be seen from Figure 7a and 7b the change in L is not seriously influencing P_2 versus P_1 plots. The reason of this observation is due to the ρ_{blp} of PE and T, and possibly shape and size d_p. On the other hand as can be seen from Figure 7c, P_2 versus P_1 variation is much more influenced by L.

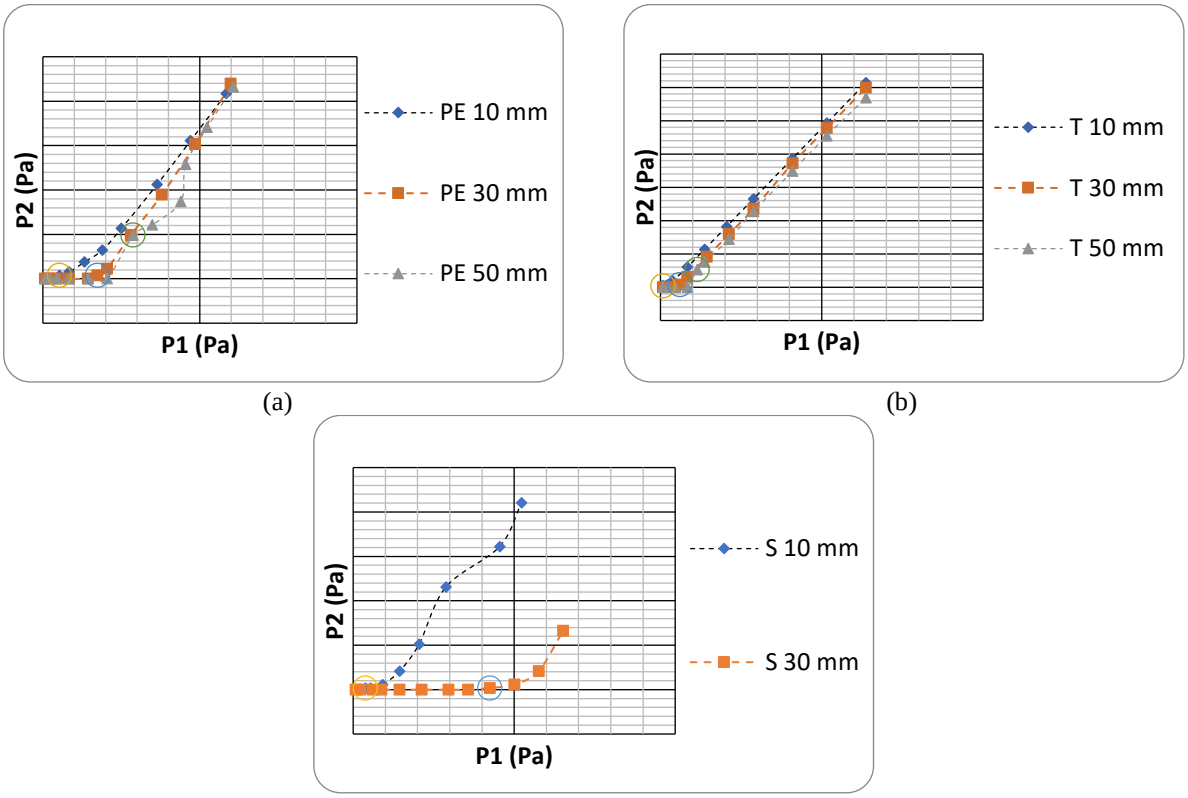

Figure 7. Minimum fluidization state change as a function of bed thickness for (a) PE, (b) T, and (c) S

In Figures 8a and 8b P_2 of Z1 and W particles are given as a function of P_1. The loose poured bulk density ρ_{blp} of Z1 is higher than that for W, but the U_{mf} of W is seen to be higher than that for Z1 at L10, L30 and L50. This may be related to the small particle size d_p of Z1 with regarding to W. SE and Z2 have same characteristics which are shown in Figure 9a and 9b. U_{mf} of the SE is less than Z2 at L10, L30 and L50 although the d_p of SE is equal to Z2 which is referred in Table 3. It seems the reason of difference may be related with ρ_{blp} values of Z2 and SE. The reason of the low U_{mf} for SE may be because of that ρ_{blp} is more effective than d_p for the determination of minimum fluidization states.

Flow modes are clearly observed in vertical test set-up. While the air flow rate is not enough to fluidize solid particles in the pipe $U_{air} << U_{mf}$, unstable zone is observed. At minimum fluidization velocity of solid particles $U_{air} = U_{mf}$, fluidized dense phase is observed and then with increasing the air flow rate, all particles are suspended in

the air flow with $U_{air} > U_{mf}$. This flow mode is called as dilute phase. So that, all flow modes are observed for covered particles in each L at vertical test set-up.

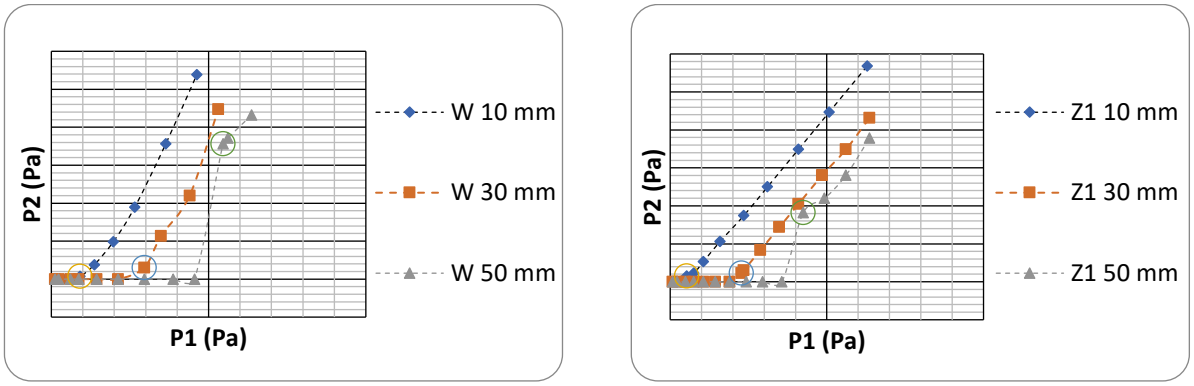

(a) (b)

Figure 8. Minimum fluidization state change as a function of bed thickness for (a) W and (b) Z1

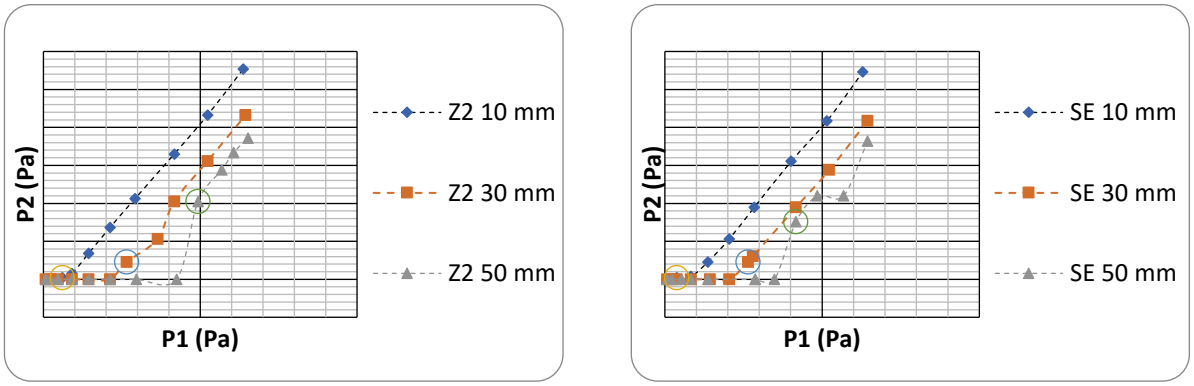

(a) (b)

Figure 9. Minimum fluidization state change as a function of bed thickness for (a) Z2 and (b) SE

3.3 Results in the Horizontal Test Set-up

In horizontal test set-up minimum fluidization velocities are given with U'_{mf}. For each test case, horizontal acrylic glass pipe is filled with mass of W, S, SE, PE and T particles as 500 gr, 1000 gr, 500 gr, 500 gr and 100 gr respectively with the use of a 10 mm diameter hole at $X_H/D=10$ from the beginning of the acrylic glass pipe until the pipe has full of particle as shown in Figure 10.

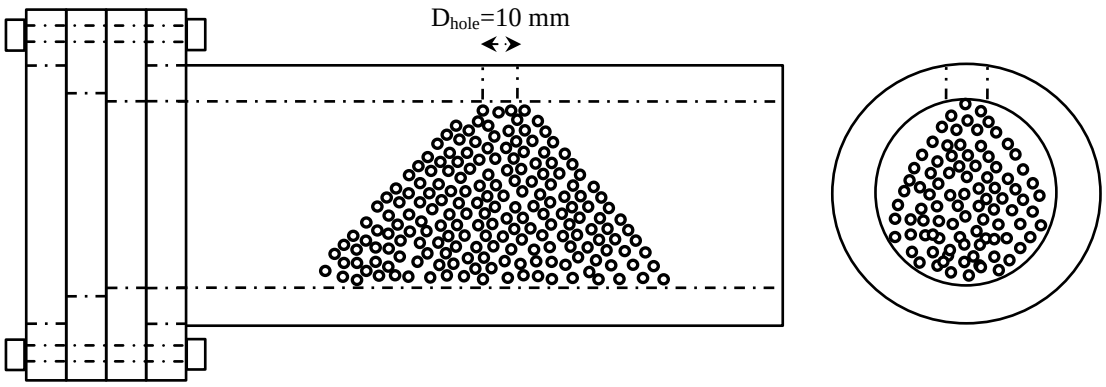

Figure 10. Horizontal test set-up with particles

U_{air} is increased and at each U_{air} field is observed. The U_{air} is taken as U'_{mf} which are given in Table 4 when the air velocity U_{air} at which first particles over the top of triangular horizontal bed carried. The carried $\dot{M}_p$ and time

are used to determine U'_{mf}. The minimum and maximum U'_{mf} are observed for SE with d_p = 700 µm and ρ_{blp} = 850 kg/m^3 at U'_{mf} = 6.99 m/s and the W with d_p = 2250 µm and ρ_{blp} = 950 kg/m^3 at U'_{mf} = 16.32 m/s. This result showed that the d_p values are dominant in comparison to ρ_{blp} to determine U'_{mf}. In addition to this, U'_{mf} of particles in horizontal test set-up are higher than U_{mf} of particles at L10 in vertical test set-up except for SE.

Table 4. U'_{mf} of W, S, SE, PE and T in horizontal test set-up

Particles	Horizontal Test Set-up U'_{mf} (m/s)
W	16.32
S	10.75
SE	6.99
PE	12.47
T	8.94

Figures from 11a to 11j illustrate a sample visual observation of each stage during a test run for PE. When the $U_{air} << U'_{mf}$ slug flow is observed as shown in the Figures 11a and 11b. U_{air} of first breaking point from the top of solid particle hill is taken as U'_{mf}. Figures from 11c to 11f showed that start to fluidization where $U'_{mf} = U_{air}$. Then, solid particles hill is transformed to a long line in the pipe shown in Figures from 11g to 11j. This long particles line is called as plug flow where $U_{air} > U'_{mf}$. Solid particles line shortens continuously depending on U_{air} before the pipe is totally discharged. At this time flow mode is observed as fully suspended- dilute phase where the $U_{air} >> U_{mf}$.

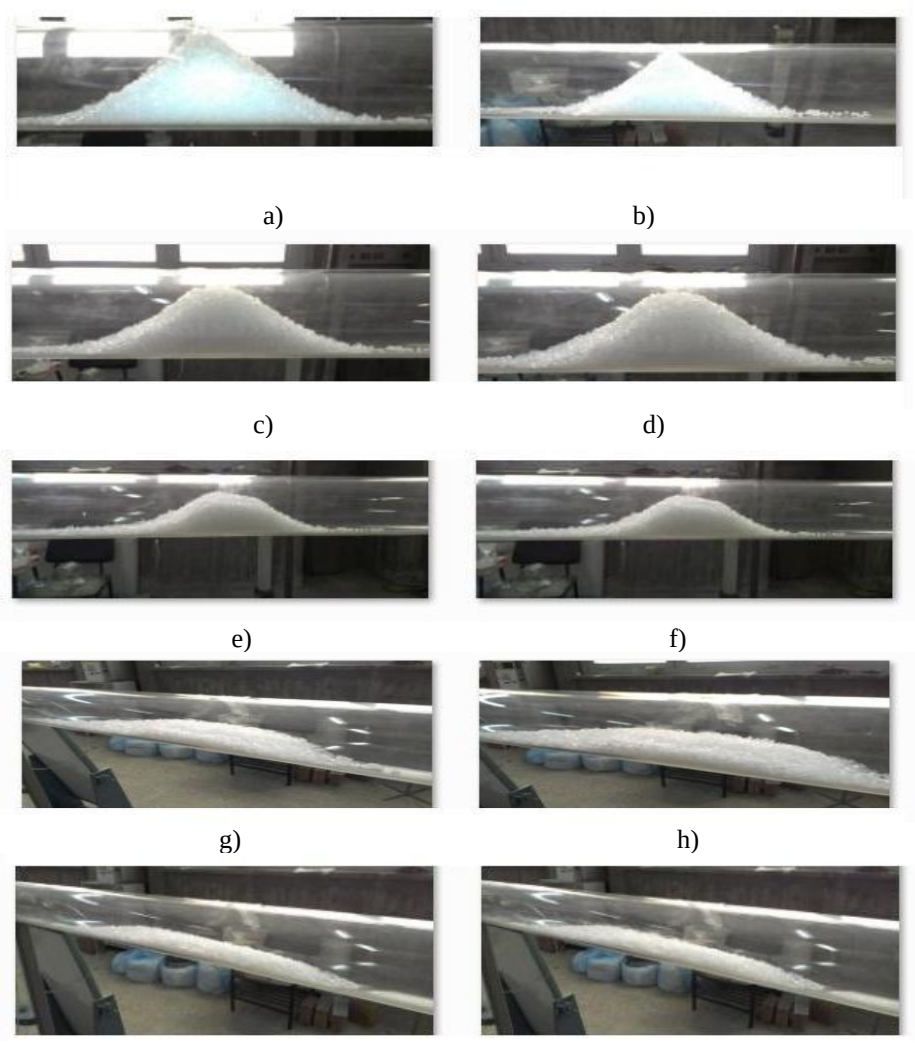

Figure 11. Visual observation of polyethylene

Figure 12 showed that the variation of P_2 versus P_1 for horizontal test set-up for five solid particles in which minimum fluidization states are marked with a circle symbol of "O". Variation of P_2 versus P_1 was used to

determine fluidization states for the vertical test set-up and it is shown the sudden increase in P_2 represented the minimum fluidization states. On the other hand, as shown in Figure 12 in horizontal test set-up, this method does not give any remarkable results to determine fluidization state similar to vertical test set-up. P_2 increases almost gradually with P_1 without a special influence of "O" point. For this reason, an alternative method is proposed.

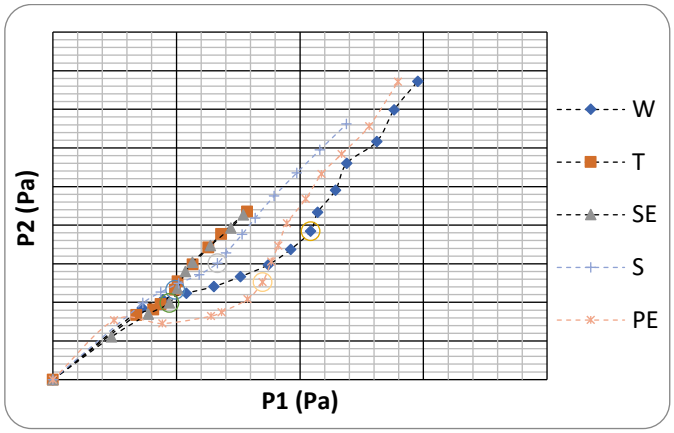

Figure 12. Pressure variation and minimum fluidization state change horizontal test set-up

Pressure drops; ΔP_2, ΔP_3 and ΔP_4 are used for the determination of states for each particle. Pressure difference of P_1 and P_2, P_1 and P_3 and P_1 and P_4 are symbolized as ΔP_2, ΔP_3 and ΔP_4. Fluidization states are shown with a circle symbol as before. The local pressure drops versus U_{air} are given in Figures from 13 to 17. In vertical test set-up; variation of local pressure magnitudes before and after the packed cylindrical material samples as a function of U_{air} is used to determine U_{mf} and its link with flow dynamics. In horizontal test set-up the similar measurement practice indicated that variation of local pressures before and after the packed triangular material samples presented a different functional relationship with U_{air} Therefore local pressure drops ΔP_2, ΔP_3 and ΔP_4 defined as the local pressure differences.

The minimum slope of local pressure drop values are shown in Figure 13 for T which has the lowest ρ_{blp} of 200 kg/m^3 in this study. This may be the reason of the lowest slope. The new expectations is the maximum slope for the particle of maximum density which is sand with ρ_{blp} of 2400 kg/m^3 with regarding this proposal. But, sand particles which has the minimum average diameter of 150 µm in this study, are not generated the maximum slope of pressure drop as shown in Figure 14. So, the slope of the pressure drop is not only related with loose pored bulk density, ρ_{blp} it is also related with average particle diameter, d_p.

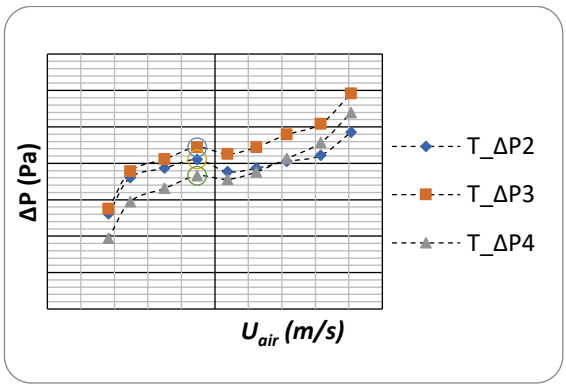

Figure 13. ΔP as a function of U_{air} for T

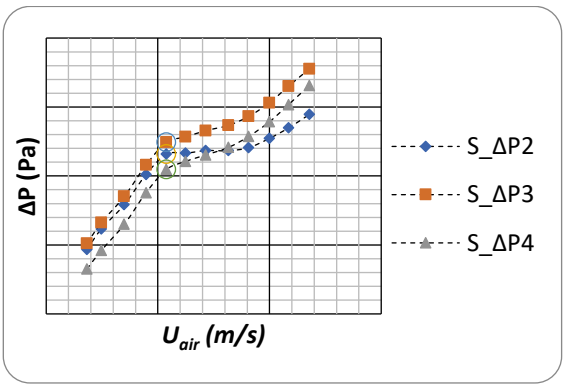

Figure 14. ΔP as a function of U_{air} for S

In Figure 15, local presure drop versus U_{air} for SE is given. In this figure, local pressure drop for SE with the maximum ΔP = 117.33 Pa. The pressure drop for W and PE are ΔP = 246.27 Pa and ΔP = 212.84 Pa, respectively as shown in Figures 16 and 17. The reason of this result may be because of the fact that the average particle diameter of SE with d_p = 700 µm is less than W and PE with d_p = 2250 µm and d_p = 2750 µm respectively.

In horizontal test set-up particles are filled into the pipe then experiment is started. This is caused to the slug flow formation in the pipe in the beginning of the experiment with U_{air} = 0. Flow field is stayed stable until the first breakaway points from the prismatic shape of particles at $U'_{mf} >> U_{air}$. After this points, particles are spreaded into the pipe, then it is provided to transition of plug flow when the $U_{air} = U'_{mf}$. Following that long plugs are occured

when the $U_{air} > U'_{mf}$ in through the pipe line and it is called as plug flow. With the increasing of U_{air} all particles are started to flow in the air flow and again plug flow is occurred at $U_{air} >> U'_{mf}$.

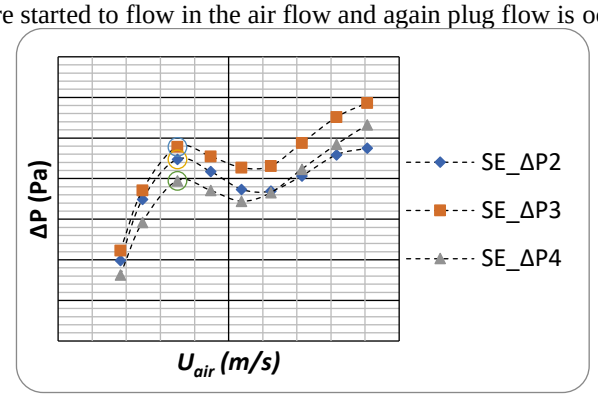

Figure 15. ΔP as a function of U_{air} for SE

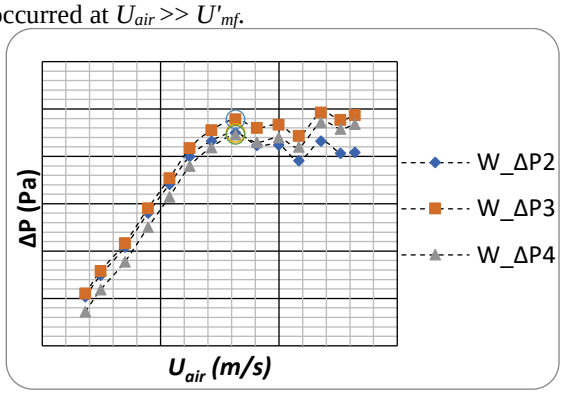

Figure 16. ΔP as a function of U_{air} for W

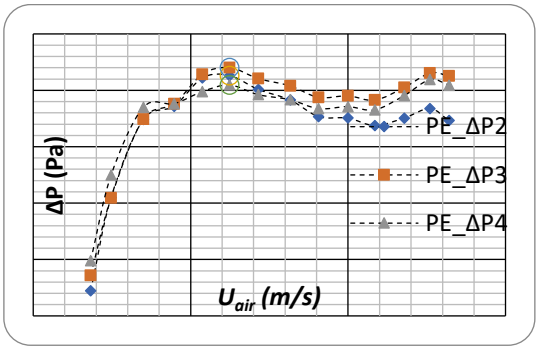

Figure 17. ΔP as a function of U_{air} for PE

3.4 Results in Continuous Conveying with Particle Feeder

In this test case, S, W and SE are used to observe flow modes during the continuous conveying with particle feeder where located at $X_H/D=0$. The particle feeder induced the known amount of particles into the pipeline system with determined mass flow rates, $\dot{m}_p$ with the ranges of 0.0149 kg/s < $\dot{m}_p$ < 0.111 kg/s. The measurements are started at the maximum U_{air} = 26.41 m/s to observe a fully suspended- dilute phase inside the horizontal test section until no particle conveying. During the process, local static pressure values are recorded at X_H/D=2, 18, 32 and 48 and also conveyed particles are weighed. The measurements are repeated by reducing U_{air} for S, W and SE particles where the U'' = 14.29 m/s, 14.29 m/s and 12.47 m/s respectively. U'' is defined as before the no particle conveying velocity in continuous conveying test section. Particle feeder having different sized orifice plates which is used to induce different $\dot{m}_p$ except for T and PE particles which is given in Table 5. U_{air}, and local pressure drop values ΔP_2, ΔP_3 and ΔP_4 are measured together with the carried mass of particles; $\dot{M}_p/\dot{M}_a$ through the experiments. Here, $\dot{M}a$ is the air mass flow rate and $\dot{M}_p$ is the mass flow rate of particles which are carried by different values of U_{air}. Mass flow rates of particles with respect to air mass flow rates are tabulated in Table 6.

In continuous conveying tests only dilute phase is observed. S particles is induced into the pipeline with the ranges of 0.5 % < $\dot{M}_p/\dot{M}_a$ < 29.14 % shown in Figure 18. ΔP ranges of S particles stated that the mass flow rates are directly related to local pressure drops in pipeline.

In Figure 18a, ΔP2, ΔP3 and ΔP4 are 77.14 Pa, 92.73 Pa and 82.11 Pa while $\dot{M}p/\dot{M}a$ = 0.5 %. It is seen that the magnitudes are increasing in Figures 18b and 18c ΔP2, ΔP3 and ΔP4 are 80.15 Pa, 93.24 Pa and 84.11 Pa respectively for $\dot{M}p/\dot{M}a$ = 0.65 % and ΔP2, ΔP3 and ΔP4 are 86.32 Pa, 115.32 Pa and 105.25 Pa for $\dot{M}p/\dot{M}a$ = 1.08 %.

SE particles are induced into the pipeline also with the ranges of 0.25 % < $\dot{M}p/\dot{M}a$ < 17.56 % which are given in Figure 19. The magnitudes are increasing in Figures 19a and 19b such that ΔP2, ΔP3 and ΔP4 are 59.12 Pa, 69.78 Pa and 64.74 Pa for $\dot{M}p/\dot{M}a$ = 0.37 % and ΔP2, ΔP3 and ΔP4 values are 63.55 Pa, 74.01 Pa and 68.06 Pa for $\dot{M}p/\dot{M}a$ = 0.43 %. W particles are also induced into the pipeline with only 15 mm and 20 mm orifice plates with the ranges of 0.38 % > $\dot{M}p/\dot{M}a$ > 12.20 %. The results are given in Figure 20. W particles are not discharged from the 10 mm orifice plate. The magnitudes are increasing in Figure 20b, namely ΔP2, ΔP3 and ΔP4 are 71.18 Pa, 79.46 Pa and 75.32 Pa for $\dot{M}p/\dot{M}a$ = 0.43 %.

Table 5. Calibration of particle feeder

Particle Mass Flow Rate, $\dot{m}_p$ (kg/s)			
	Orifice Diameters		
Material	10 mm	15 mm	20 mm
Z1	0.0061	0.0163	0.0294
Z2	0.0055	0.0108	0.0252
W	-	0.0166	0.0250
SE	0.0149	0.0312	0.0434
S	0.0285	0.0566	0.1111

Table 6. Mass flow rates of particles with respect to air for continuous conveying

Particle	Orifice (mm)	Max $\dot{M}_p/\dot{M}_a$ (%)	Min $\dot{M}_p/\dot{M}_a$ (%)
W	20	12.2	0.43
	15	9.47	0.38
S	20	29.14	1.08
	15	23.74	0.65
	10	14.2	0.5
SE	20	17.56	0.43
	15	11.7	0.37
	10	4.18	0.25

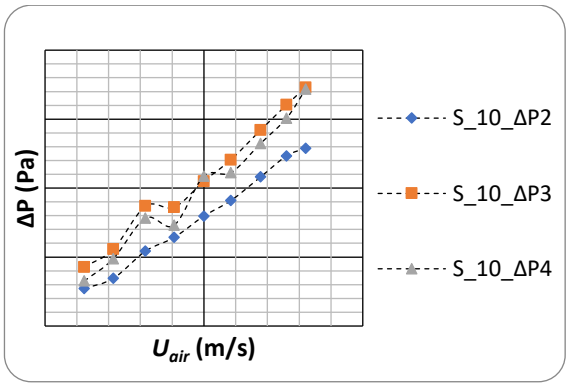

(a)

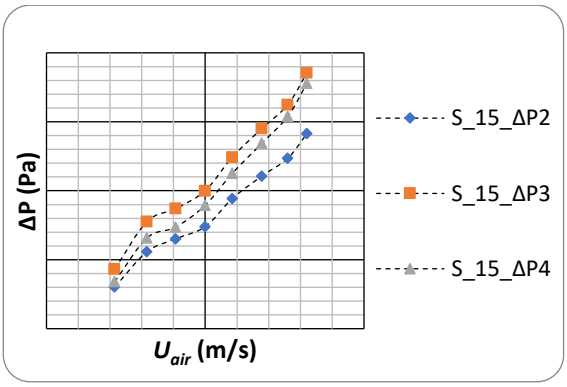

(b)

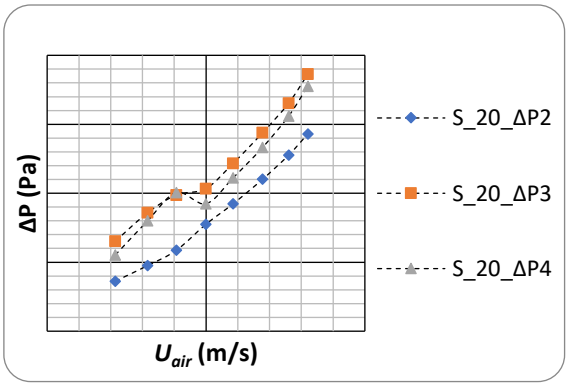

(c)

Figure 18. ΔP as a function of U_{air} for S particles with the range of (a) $0.50 < \dot{M}_p/\dot{M}_a < 14.20$, (b) $0.65 < \dot{M}_p/\dot{M}_a < 23.74$, and (c) $1.08 < \dot{M}_p/\dot{M}_a < 29.14$

For the general view of the link between the local pressure drop and Ṁp/Ṁa for S, W and SE particles, they are in the similar characteristics. ΔP increases as Ṁp/Ṁa increases. However, local pressure drop values are differently affected by solid particles because of their ρblp and dp. Due to their small size, SE particles generated lower local pressure drop values in comparison to W particles for the same Ṁp/Ṁa = 0.43 %. On the other hand the local

pressure drop values for S at Ṁp/Ṁa = 5.33 % are seen to be higher than that for SE at Ṁp/Ṁa = 5.44 %. Local pressure drop values are given ΔP2, ΔP3 and ΔP4 as 114.22 Pa, 136.09 Pa, 123.05 Pa (for S) and 88.50 Pa, 109.21 Pa, 99.46 Pa (for SE) which is predicted due to ρblp of S is higher than that of SE.

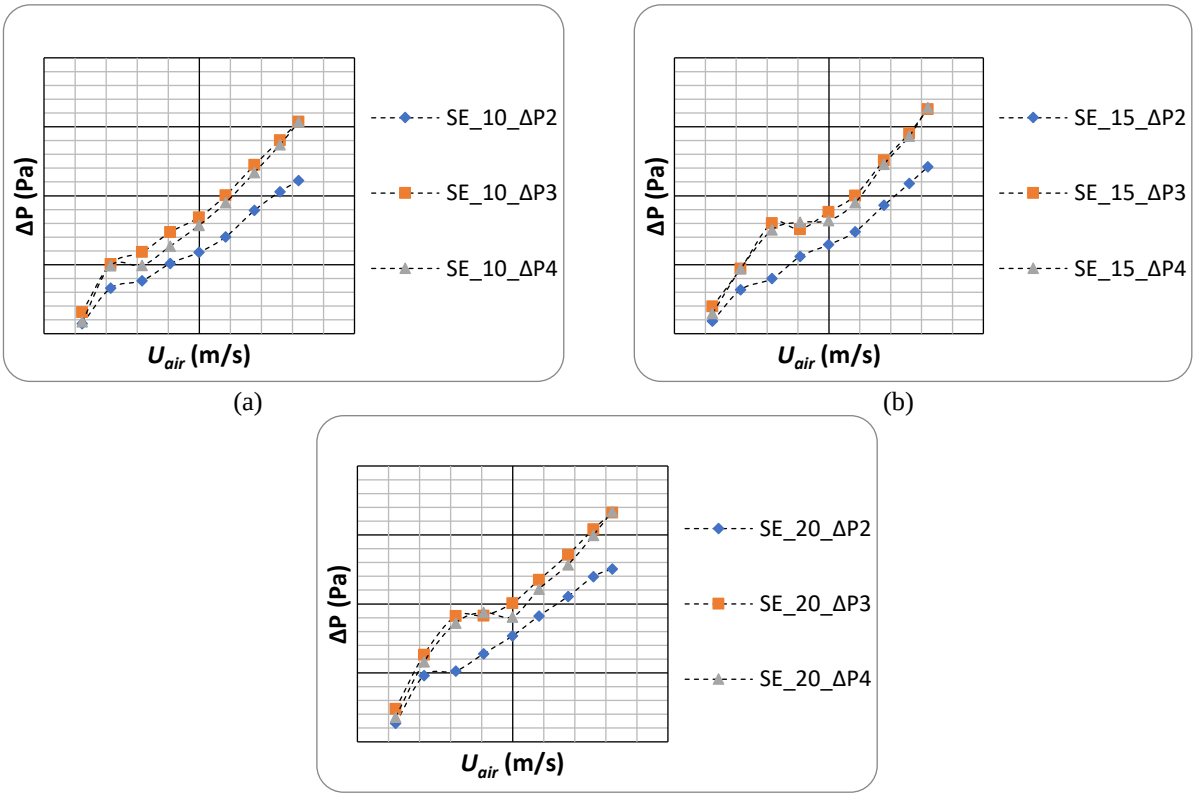

Figure 19. ΔP as a function of U_{air} for SE particles with the range of (a) 0.25 < Ṁp/Ṁa < 4.18, (b) 0.37 < Ṁp/Ṁa <11.70, and (c) 0.43 < Ṁp/Ṁa < 17.56

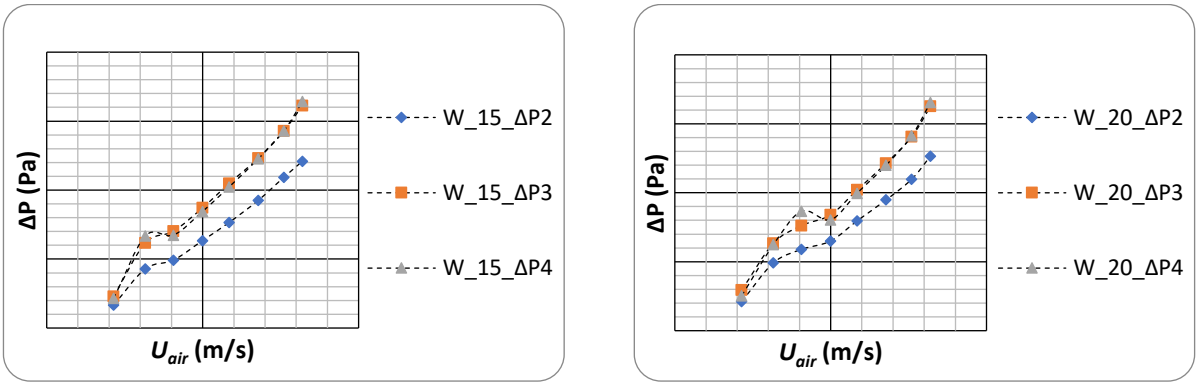

Figure 20. ΔP as a function of U_{air} for W particles with the range of (a) 0.38 < Ṁp/Ṁa < 9.47 and (b) 0.43 < Ṁp/Ṁa < 12.20

4 CONCLUSION

In this paper three different cases which are vertical (test case 1), horizontal (test case 2) and continuous conveying test case are used to determine flow modes in pneumatic conveying systems. Seven solid particles which are SE, W, S, T, PE, Z1 and Z2 with the range of 200 kg/m^3 < ρ_{blp} < 2400 kg/ m^3 and 150 µm < d_p < 2750 µm are used in these three cases. The used parameters are calculated with the ranges of 17714 < Re$_{mf}$ < 147600, 3.65 m/s < U_{mf} < 24.83 m/s, 0.0052 m2/Pa.s < P_f < 0.92 m2/Pa.s and 0.25 % < Ṁp/Ṁa < 51.99 %.

In vertical test set-up unstable zone and fluidized dense phase is occurred, then in the horizontal test set-up slug flow and plug flow is observed and lastly plug flow and dilute phase is occurred visually in continuous conveying

test case. Finally, all obtained data which are explained in the previous sections are classified according to flow modes in pneumatic conveying systems. The flow modes are given as boundaries of flow modes in Table 7 with regarding to three test cases which are vertical, horizontal, and continuous.

An increase of loose poured bulk density, ρ_{blp} causes an increase of minimum fluidization velocity, U_{mf} in vertical test set-up. On the other hand, increase of average particle diameter, d_p causes an increase of minimum fluidization velocity in horizontal test set-up. Furthermore, the average particle diameter is seen to be more effective in horizontal test set-up in comparison with vertical one. These deductions on ρ_{blp}, d_p are due to the constraints at horizontal and vertical test cases.

As a result of the study, some further investigations on the manner will be conducted as follows:
- The particle characteristics should be considered particularly for the ranges of $d_p < 100$ μm and $d_p > 3000$ μm.
- The range of study should be extended to cover of a variety of industrial applications.
- The constructed test system should be revised to have a fully automated structure.

Table 7. Boundaries of flow modes in three test cases

Vertical Test Set-up			
Unstable Zone	Transition of Fluidized Dense Phase	Fluidized Dense Phase	
$U_{air} << U_{mf}$	$U_{air} = U_{mf}$	$U_{air} > U_{mf}$	$U_{air} >> U_{mf}$
Horizontal Test Set-up			
Slug Flow	Transition of Plug Flow	Plug Flow	
$U_{air} << U'_{mf}$	$U_{air} = U'_{mf}$	$U_{air} > U'_{mf}$	$U_{air} >> U'_{mf}$
Continuous Conveying Test Set-up			
Plug Flow		Dilute Phase	
$U_{air} \leq U''$		$U_{air} >> U''$	

Acknowledgments
The authors would like to thank Gaziantep University, BAPYB- The Scientific Research Projects Governing Unit for the project under the grant number of MF.12.15.

Author Contributions
Alperen TOZLU: Conceptualization, Methodology, Software, Investigation, Resources, Writing - Original Draft, Writing - Review & Editing, Visualization
Ahmet İhsan KUTLAR: Writing - Review & Editing, Visualization, Supervision
Melda ÇARPINLIOĞLU: Conceptualization, Methodology, Validation, Writing - Original Draft, Writing - Review & Editing, Supervision

All authors read and approved the final manuscript.

Conflict of interest
No conflict of interest was declared by the authors.

References

[1] D. Geldart, “Types of Gas Fluidization,” *Powder Technology*, vol.7, pp. 285-292, 1973.

[2] D. Geldart, *Powder Technology*, vol. 6, pp. 201, 1972.

[3] G. Dixon, “The Impact of Powder Properties on Dense Phase Flow,” *In Proceedings of the international conference on pneumatic conveying*, 1979.

[4] O Molerus, “*Proc. Intern. Symp. on Fluidization*,” Eindhoven, Netherlands Univ. Press Amsterdam, 1967.

[5] O. Molerus, “Interpretation of Geldart’s Type A, B, C and D Powders Taking into Account Interparticle Cohesion Force,” *Powder Technology*, vol. 33, pp. 81-87, 1982.

[6] O. Molerus, “*Chem. Engng. Science 35*,” Vol. 6, pp. 1331, 1980.

[7] N. J. Mainwaring, A.R. Reed, “Permeability and Air Retention Characteristics of Bulk Solid Materials in Relation to Modes of Dense Phase Pneumatic Conveying,” *Bulk Solids Handling*, vol. 7(3), pp. 415-425, 1987.

[8] C. Fargette, M.G. Jones, G. Nussbaum, "Bench Scale Tests Assessment of Pneumatic Conveying Behavior of Powders," *Powder Handling and Processing*, vol. 9(2), pp. 103-110, 1997.

[9] L. Sanchez, N. Vasquez, G. E. Klinzing, S. Dhopdakar, "Characterization of Bulk Solids to Assess Dense Phase Pneumatic Conveying," *Powder Technology*, vol. 138, pp. 93-117, 2003.

[10] R. Pan, P. Wypych, I. Frew, "*6th Intl. Conf. on Bulk Materials, Storage, Handling and Transport*," Wollongong, AU, September, 1998.

[11] R. Pan, I. Frew, D. Cook, "*I-Mechanical Engineering*," 65 (C566/044/2000).

[12] R. Pan, "Intl. Conf. on Bulk Materials," *Storage, Handling and Transport*, Newcastle, AU, July, 1995.

[13] R. Pan, "Material Properties and Flow Modes in Pneumatic Conveying," *Powder Technology*, vol. 104, pp. 157-163, 1999.

[14] K. C. Williams, M. G. Jones, "Classification Diagrams for Dense-Phase Pneumatic Conveying," *Powder Handling and Processing*, vol. 15(6), pp. 368-373, 2003.

[15] M. G. Jones, K. C. Williams, "Predicting the Mode of Flow in Pneumatic Conveying Systems," *Particuology*, vol. 6, pp. 289-300, 2008.

[16] R. Jackson, "*Trans. Inst. Chem. Engrs*," vol. 41, pp. 13, 1963.

[17] R L. Pigford, T. Baron, "*Ind. Eng. Chem. Fundamentals*," vol. 4, pp. 81, 1965.

[18] L. Davies, J. F. Richardson, "*Transactions of the Institution of Chemical Engineers*," vol. 44, T293, 1966.

[19] H. Rumpf, "*Chemie-kg-Technik*," vol. 42, pp. 538, 1970.

[20] H. Krupp, "*Adv. in Coil. and Interf. Sci*," vol. 1, pp. 2, 1967.

[21] K. B. Mathur, "Chapter 17. Spouted Beds, in Davidson J.F., and Harrison D. H. Fluidization," *Academic Press*, London and Newyork, 1971.

[22] A. J. Chambers, S. Keys, R. Pan, "The Influence of Material Properties on Conveying Characteristics," *In Proceedings of the 6th international conference on bulk materials storage, handling and transportation*, pp. 309-319, 1998.

[23] M. G. Jones, U. K. Mills, "Product classification for pneumatic conveying," *Powder Handling and Processing*, Vol. 2, pp. 117–122, 1990.

[24] B. Mi, "Low Velocity Pneumatic Transportation of Bulk Solids," PhD Dissertation, Wollongong University, AU, 1994.

[25] O. C. Kennedy, "*6th International Conference on Bulk Materials Storage, Handling and Transportation*," Wollongong, Australia, 8 – 30 September, 1998.

[26] D. Geldart, A. C. Y. Wong, "*Chemical Engineering Science*" Vol. 40, pp. 653–661, 1985.

[27] M. Kwauk, "Fluidization: Idealized and Bubbleless, with Applications," *Ellis Horwood*, New York, 1992.

[28] L. Sanchez, "Characterization of Bulk Solids for Dense Phase Pneumatic Conveying," MS Thesis, University of Pittsburgh, 2001.

[29] S. Ergun, "Fluid Flow Through Packed Columns," *Chemical Engineering Progress*, vol. 48, pp. 89-94, 1952.

[30] A. Tozlu, E. Özahi, A. İ. Kutlar, M. Ö. Çarpınlıoğlu, "Modes of Flow in Pneumatic Conveying Systems," *FLUIDS-HEAT'12, Recent Researches in Applied Mechanics*, Greece, vol. 1, pp. 51-57, March, 2012.

[31] A. Tozlu, M. Ö. Çarpınlıoğlu, "An Experimental Test Set-up and the Range of Study for Determination of Flow Modes in Pneumatic Conveying Systems," *Recent Advances in Continuum Mechanics Hydrology and Ecology*, Rhodes Islands, vol.14, pp. 61-66, 2013.

[32] M. Ö. Çarpınlıoğlu, "An Analysis of Flow Mechanics through Packed-Fluidized Beds of a Variety of Solid Particles: A Methodology for the Determination of Flow Modes in Pneumatic Conveying Systems," *Recent Advances in Continuum Mechanics Hydrology and Ecology*, Rhodes Islands, vol.14, pp. 71-76, 2013.

[33] M. Ö. Çarpınlıoğlu, "An analysis on flow modes in pneumatic transport lines, Project Report," BAP University of Gaziantep MF 12.05, 2014.

[34] A. Tozlu, "An Analysis on Flow Modes in Pneumatic Conveying Systems," M.Sc. Thesis, University of Gaziantep, 2014.

[35] ANSI/ASME PTC 19.1-1985 Part 1, Measurement Uncertainty (Available from ASME Order Dept., 22 Law Drive, Box 2300, Fairfield, New Jersey 07007-2300), 1986.